Square Patterns in Rayleigh-Bénard Convection with Rotation about a Vertical Axis

Kapil M. S. Bajaj, Jun Liu, Brian Naberhuis, and Guenter Ahlers
Department of Physics and Center for Nonlinear Science, University of California, Santa Barbara, California 93106
(Received 26 January 1998)

We present experimental results for Rayleigh-Bénard convection with rotation about a vertical axis at dimensionless rotation rates $0 \leq \Omega \leq 250$ and $\epsilon \equiv \Delta T/\Delta T_c - 1 \lesssim 0.2$. Critical Rayleigh numbers and wave numbers agree with predictions of linear-stability analysis. For $\Omega \gtrsim 70$ and small ϵ the patterns are cellular with local fourfold coordination and differ from the theoretically expected Küppers-Lortz unstable state. Stable as well as intermittent defect-free square lattices exist over certain parameter ranges. Over other ranges defects dynamically disrupt the lattice but cellular flow and local fourfold coordination is maintained. [S0031-9007(98)06696-4]

PACS numbers: 47.54.+r, 47.20.Lz, 47.27.Te

The elucidation of spatiotemporal chaos (STC) remains one of the major tasks in the study of pattern formation in nonlinear dissipative systems [1]. The best opportunities for theoretical understanding of experimental observations of a chaotic state exist when the mean-square amplitude of STC evolves continuously (i.e., via a supercritical bifurcation) from a spatially uniform ground state; for in that case it should be possible at least in principle to derive from the equations of motion of the system a systematic, simplified description in the form of Ginzburg-Landau equations. However, experimentally accessible supercritical bifurcations from the uniform state to STC are rare because most systems with supercritical primary bifurcations become variational as the threshold is approached from above and thus approach a time-independent state. Convection in a shallow horizontal layer of a fluid heated from below (Rayleigh-Bénard convection or RBC) and rotated about a vertical axis is one of the exceptions. Convection occurs when the temperature difference ΔT exceeds a critical value $\Delta T_c(\Omega)$ (Ω is the rotation frequency) and leads to a velocity field $\mathbf{v}$. The Coriolis force $\mathbf{\Omega} \times \mathbf{v}$ renders the system nonvariational and thus permits the existence of STC at onset. Küppers and Lortz (KL) [2] predicted that a primary supercritical bifurcation leads to a state of unstable convection rolls provided $\Omega > \Omega_{\mathrm{KL}}$. In this KL state, rolls of one orientation are unstable with respect to another set of rolls with an angular orientation relative to the first which is advanced in the direction of rotation by an angle θ [2–4]. The new set, however, is equally unstable to yet another, and so forth. Several experiments found the KL state at relatively large $\epsilon \equiv \Delta T/\Delta T_c - 1$ [5–7]. Recent ones [8–11] have shown its existence close to threshold for $\Omega_{\mathrm{KL}} \simeq 12 \lesssim \Omega \lesssim 20$ and have verified the supercritical nature of the bifurcation. The instability was observed to lead to a chaotically time-dependent coexistence of domains with different roll orientations. Two examples [11] of this domain chaos are shown in Figs. 1a and 1b.

Theoretically it is expected [2–4,12] that the nature of the bifurcation and of the nonlinear state above it should remain qualitatively unchanged as Ω is increased. We show that this is not the case. For $\Omega \equiv 2\pi f d^2/\nu \gtrsim 70$

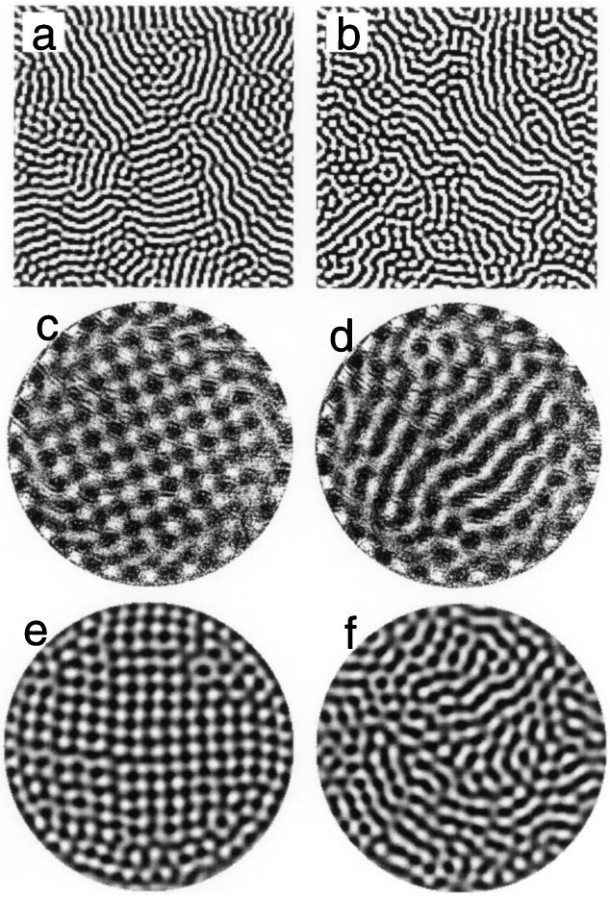

FIG. 1. Shadowgraph images of convection patterns viewed from above for CO_2 [(a) and (b), only parts of patterns are shown; adapted from Ref. [11]], water [(c) and (d), the entire cell is shown], and argon [(e) and (f), 90% of the cell radius is shown], with (σ, Ω, Γ) equal to (0.93, 19.8, 40), (5.4, 170, 4.8), and (0.69, 181, 8.3), respectively. For small Ω [(a),(b)] the patterns have domains which are typical of the KL instability for all ϵ near zero, as illustrated for $\epsilon = 0.06$ (a) and 0.18 (b). At larger Ω, square patterns occur close to onset [(c) $\epsilon = 0.09$ and (e) $\epsilon = 0.04$], but states similar to the KL domains are observed for $\epsilon \gtrsim 0.1$ [$\epsilon = 0.12$ in (d) and $\epsilon = 0.13$ in (f)]. In (c) and (d), the cells along the periphery are the wall mode.

 0031-9007/98/81(4)/806(4)$15.00

(f is the rotation frequency in Hz and ν the kinematic viscosity) the bifurcation does remain supercritical, but the convection pattern close to onset has no similarity to the expected KL state. Instead the pattern consists of cells which are usually arranged so as to have local fourfold coordination. Over significant parameter ranges the cells "crystallize" and form a slowly rotating square lattice [13]. Typical examples are shown in Figs. 1c and 1e. They differ dramatically from the expected patterns illustrated in Fig. 1a. Depending on the parameters, the lattice can be stable, can be intermittently disrupted by defects, or can be continuously disordered with many defects within it (maintaining, however, the cellular character with predominantly local fourfold coordination). At larger ϵ ($\epsilon \gtrsim 0.1$), we observe patterns reminiscent of the KL state, as illustrated in Figs. 1d and 1f. The square pattern for ϵ values below those where the KL state is observed is contrary to the prediction [2–4,12].

One may ask whether the known idealizations in the theory (the Boussinesq approximation, neglect of the centrifugal force, and the assumption of an infinitely extended system) could be responsible for the difference between experiment and theory. We show below that Q (the size of departures from the Boussinesq approximation) and the Froude number F (the relative importance of centrifugal forces) are small in the experiments. We also varied Q and F over significant ranges and used two different aspect ratios Γ. The unexpected cellular flow and square lattices occurred under all of these conditions over about the same ranges of ϵ and Ω. Thus we have no evidence for the importance of the effects neglected in the theory. We also emphasize that the observed cellular flow persists over about the same Ω and ϵ range when the Prandtl number σ is varied from 0.7 to 5.

We used water and argon with $\sigma \equiv \nu/\kappa$ (κ is the thermal diffusivity) of 5.4 and 0.69, respectively, in two different apparatus [14,15]. The temperatures of the tops of the cells were regulated to ± 1 mK at 30.07 °C (water) and at 37.5 °C (argon). Aspect ratios $\Gamma \equiv r/d = 4.8$ and 8.3 (r is the radius and d the height of the fluid layer) were used for water ($r = 38.1$ mm, $d = 7.9$ mm) and argon ($r = 33.2$ mm, $d = 4.0$ mm), respectively. The apparatus were rigidly mounted on rotating tables capable of rotation up to $f = 1$ Hz, covering the range $0 \leq \Omega \leq 250$. Shadowgraph assemblies were mounted on top of the convection apparatus to obtain images in the rotating frame. For argon, the pressure was controlled to ± 2 mbar. The experiments were carried out by raising the bottom-plate temperatures at fixed Ω. Both heat-transport measurements and shadowgraph images were taken after waiting for at least a horizontal diffusion time $\tau_h = \Gamma^2 d^2/\kappa$. Onset was determined both from the heat transport and from amplitudes of the shadowgraph images [16]. Wave numbers were obtained from Fourier transforms of the patterns.

The dimensionless control parameters are the Rayleigh number $R \equiv \alpha g d^3 \Delta T/\kappa\nu$ and Ω. Here α is the isobaric thermal expansion coefficient, g the acceleration due to gravity, and ΔT the temperature difference across the cell. The Froude number $F \equiv 4\pi^2 f^2 r/g$ is less than 0.03 in most of the experiments and maximally 0.12 for a few runs. Since Ω is scaled by $\tau_\nu \equiv d^2/\nu$, increasing the pressure P of argon increased Ω because it decreased ν. We used this to vary Ω by a factor of 4 at fixed f (and thus F). Increasing P changed σ only from 0.68 at 20 bar to 0.695 at 40 bar. The parameter Q [17] is proportional to $\Delta T_c(\Omega)$. For argon, $P = 20$ bar (40 bar), and $\Omega = 91$ (249), for instance, $Q = 0.15$ (0.13). For water and $\Omega = 170$, $Q \simeq -0.2$.

Figure 2 summarizes measurements of the critical Rayleigh numbers $R_c(\Omega)$ and wave numbers $k_c(\Omega)$ for the sample interiors (bulk mode) [16]. The results agree with linear-stability predictions for a laterally infinite system [18] (solid lines in Fig. 2). For $\Omega \gtrsim 70$, this onset is preceded by a "wall mode" consisting of a wave traveling (in the rotating frame) in the direction opposite to Ω [19]. This mode persists above R_c, and can be seen in Figs. 1c and 1d. The object of the present paper is the bulk mode.

Figure 3 shows shadowgraph images for $\epsilon = 0.04$ for various Ω in argon. At small Ω (Fig. 3a) the contrast of the image is poor because ΔT and the wave number were small. Nonetheless one can see that almost the

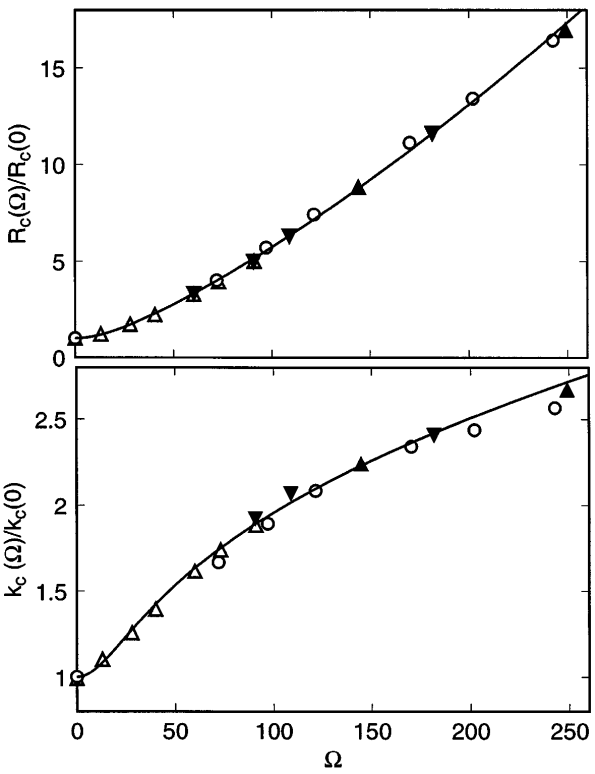

FIG. 2. The critical Rayleigh numbers $R_c(\Omega)/R_c(0)$ (top) and wave numbers $k_c(\Omega)/k_c(0)$ (bottom) as a function of Ω for water ($\sigma = 5.4$, open circles) and argon at 20 bar ($\sigma = 0.68$, open triangles), 30 bar ($\sigma = 0.69$, inverted solid triangles), and 40 bar ($\sigma = 0.695$, solid triangles). The results agree with the predictions for a laterally infinite system (solid lines) [18].

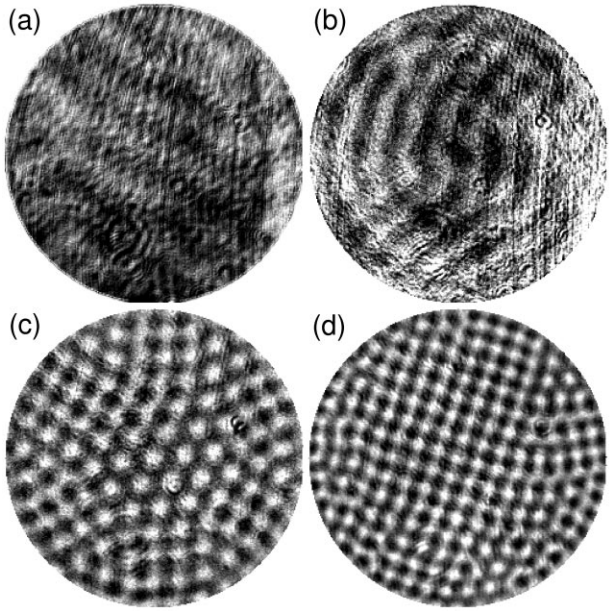

FIG. 3. Patterns for argon and various Ω at $\epsilon \simeq 0.04$. Ω values are (a) 13, (b) 40, (c) 73, and (d) 145. Only 90% of the cell radius is shown. (c) and (d) are at the same physical rotation rate and at different pressures.

entire cell was occupied by a single domain of rolls. However, the time dependence of the pattern involved switching between different domain orientations which is characteristic of the dynamics of the KL state [10,11]. At somewhat larger Ω (Fig. 3b) several KL domains exist simultaneously in the cell, as seen previously [10,11] using larger Γ and $\Omega \lesssim 20$. This situation changes when Ω is increased beyond about 70, as illustrated by Figs. 3c and 3d. For $\Omega = 73$, the pattern is cellular. There are domains where the pattern has square symmetry. Six domains meet in the cell center and locally enforce a sixfold symmetry, maintaining, however, the cellular character. At larger $\Omega = 145$ the pattern consists of a square lattice, with some domain walls and defects.

There are ranges of Ω, ϵ, and σ over which the patterns near onset were dynamically disrupted by many defects, although cellular flow, often with local fourfold coordination, was maintained. Two examples are shown in Fig. 4. In order to study the pattern dynamics in greater detail, we examined the time evolution of the structure function $S(\mathbf{k})$ (the square of the modulus of the Fourier transform). Two examples are shown in Fig. 5. The right one is typical of the KL state, whereas the left one represents a square lattice. For $\Omega = 170$ and $\sigma = 5.4$,

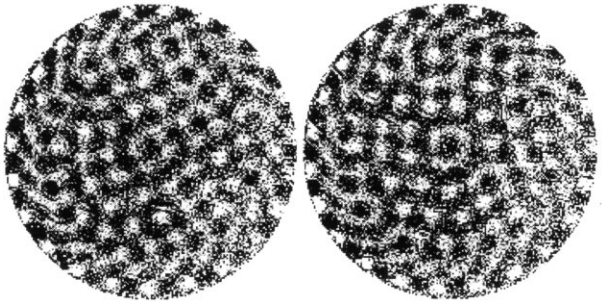

FIG. 4. Disordered cellular patterns for $\sigma = 5.4$, $\Omega = 170$, and $\epsilon = 0.052$. The entire cell is shown. Along its periphery is the wall mode.

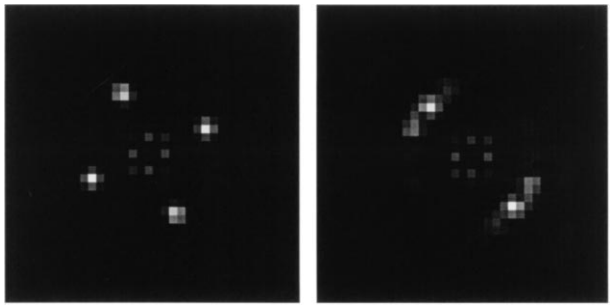

FIG. 5. Structure functions of images 1c (left) and 1d (right).

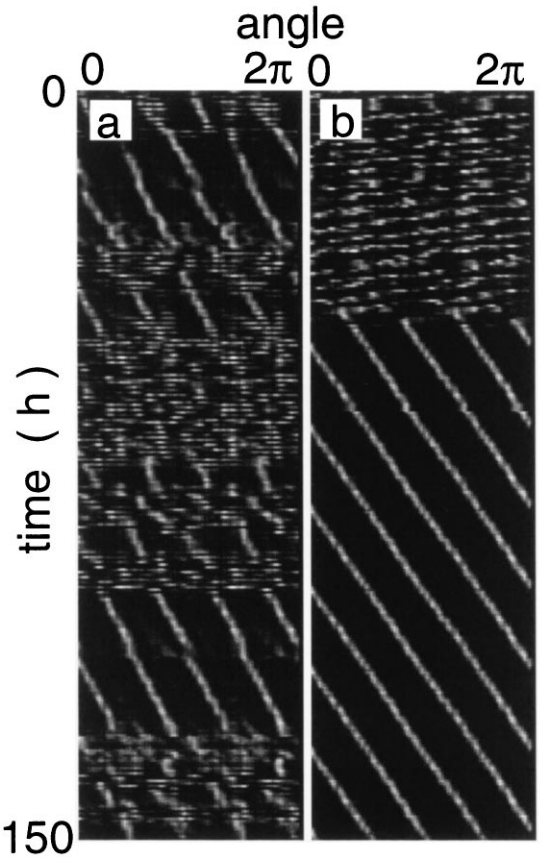

FIG. 6. Angle-time plot for the radial average of the structure function for $\sigma = 5.4$ at $\Omega = 170$ for (a) $\epsilon = 0.072$ and (b) $\epsilon = 0.091$. (a) is a representative section of a longer run. The system intermittently changes between a perfect square lattice and a disordered pattern with local fourfold coordination. For (b) ϵ was stepped from 0.14 where the pattern was disordered (KL-like) to 0.091 at time $t = -3$ h. After about $16\tau_h$, the system spontaneously chose the perfect-square pattern which then persisted for more than $38\tau_h$.

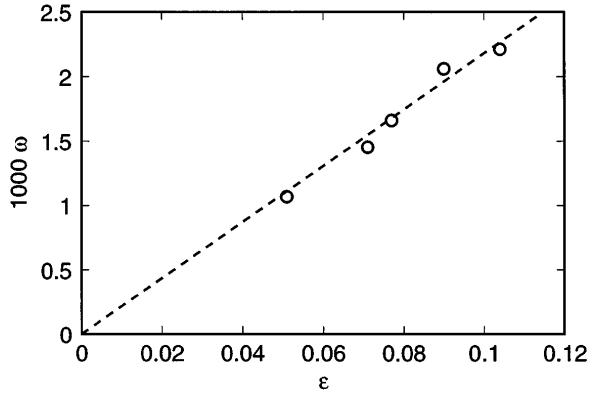

FIG. 7. The rotation rate ω of the square lattice for $\Omega = 170$ and $\sigma = 5.4$. Time is scaled by d^2/ν.

the radial average $S(\Theta)$ of $S(\mathbf{k})$ is shown in Fig. 6 as a function of time. Figure 6a is a section of a long run at $\epsilon = 0.072$. Disordered regions alternate irregularly with well ordered rotating square lattices. Figure 6b is the result of an experiment where the system was kept in the KL regime at $\epsilon = 0.14$ for a long time, and where at time $t = -3$ h ϵ was reduced to 0.091. The system remained KL-like for nearly 44 h (about 16 horizontal thermal diffusion times), and then *suddenly* crystallized into a square lattice which remained stable thereafter.

The square lattice, whenever it exists, rotates at a rate ω relative to the cell in the direction of the overall rotation Ω. Results for ω are given in Fig. 7 (for ω, time is scaled by d^2/ν). They suggest that ω vanishes at $\epsilon = 0$, as indicated by the dashed line. Presumably the rotation is a property of the finite system, and $\omega(\epsilon, \Gamma) \to 0$ as $\Gamma \to \infty$, but measurements of ω as a function of Γ have not yet been made. Under similar conditions the wall mode is traveling much faster in the opposite direction with $\omega_w \simeq -0.15$, nearly independent of ϵ.

Stable square patterns near onset occur under other conditions in RBC. Pure-fluid convection in a cell with insulating top and bottom plates [20] and binary-fluid convection with small Lewis numbers and a positive separation ratio [21] are two such systems. However, in those cases the critical wave number is reduced. Our critical wave numbers agree with the linear stability analysis for rotating RBC of a pure fluid with conducting top and bottom boundaries. Our boundaries have conductivities which are orders of magnitude larger than those of the fluids. Our argon samples, even if they were contaminated with another component, would have Lewis numbers of order one [22] and thus would not produce a square pattern due to mixture effects. Clearly impurities or poorly conducting boundaries cannot be invoked to explain our observations. Thus the occurrence of square patterns in rotating RBC at small ϵ is unexplained, and we conclude that a real discrepancy exists between theory [2–4] and experiment.

We are grateful for stimulating discussions with F.H. Busse and W. Pesch. This work was supported by U.S. Department of Energy Grant No. DE-FG03-87ER13738.

[1] M. C. Cross and P. C. Hohenberg, Rev. Mod. Phys. **65**, 851 (1993).
[2] G. Küppers and D. Lortz, J. Fluid Mech. **35**, 609 (1969).
[3] G. Küppers, Phys. Lett. **32A**, 7 (1970).
[4] R. Clever and F. H. Busse, J. Fluid Mech. **94**, 609 (1979).
[5] H. E. Heikes, Ph.D. dissertation, University of California, Los Angeles, 1979 (unpublished).
[6] F. H. Busse and K. E. Heikes, Science **208**, 173 (1980).
[7] F. Zhong, R. E. Ecke,V. Steinberg, Physica (Amsterdam) **51D**, 596 (1991).
[8] J. J. Niemela and R. J. Donnelly, Phys. Rev. Lett. **57**, 2524 (1986).
[9] E. Bodenschatz, D. S. Cannell, R. Ecke, Y. C. Hu, K. Lerman, and G. Ahlers, Physica (Amsterdam) **61D**, 77 (1992).
[10] Y.-C. Hu, R. E. Ecke, and G. Ahlers, Phys. Rev. Lett. **74**, 5040 (1995).
[11] Y.-C. Hu, W. Pesch, G. Ahlers, and R. E. Ecke (to be published).
[12] F. Busse (private communication).
[13] A square pattern near onset was observed indirectly by Heikes (Ref. [5]). However, that work did not have the optical resolution needed for direct observations. Instead, the system was equilibrated at small ϵ, and then stepped to $\epsilon = \mathcal{O}(1)$. The rapidly growing amplitude then became observable, and suggested that the pattern at the previous steady state had been one of squares. To our knowledge these observations were never reported in the published literature.
[14] G. Ahlers, D. S. Cannell, L. I. Berge, and S. Sakurai, Phys. Rev. E **49**, 545 (1994).
[15] J. R. deBruyn, E. Bodenschatz, S. Morris, S. Trainoff, Y.-C. Hu, D. S. Cannell, and G. Ahlers, Rev. Sci. Instrum. **67**, 2043 (1996).
[16] See, for instance, Y.-C. Hu, R. E. Ecke, and G. Ahlers, Phys. Rev. E **55**, 6928 (1997); **48**, 4399 (1993).
[17] F. Busse, J. Fluid Mech. **30**, 625 (1967).
[18] S. Chandrasekhar, Proc. R. Soc. London A **217**, 306 (1953); *Hydrodynamics and Hydromagnetic Stability* (Oxford University Press, London, 1961).
[19] F. Zhong, R. E. Ecke, and V. Steinberg, Phys. Rev. Lett. **67**, 2473 (1991); J. Fluid Mech. **249**, 135 (1993); R. E. Ecke, F. Zhong, and E. Knobloch, Europhys. Lett. **19**, 177 (1992); L. Ning and R. E. Ecke, Phys. Rev. E **47**, 3326 (1993); Y. Liu and R. E. Ecke, Phys. Rev. Lett. **78**, 4391 (1997).
[20] F. H. Busse and N. Riahi, J. Fluid Mech. **96**, 243 (1980); M. R. E. Proctor, J. Fluid Mech. **113**, 469 (1981).
[21] E. Moses and V. Steinberg, Phys. Rev. A **43**, 707 (1991); M. A. Dominguez-Lerma, G. Ahlers, and D. S. Cannell, Phys. Rev. E **52**, 6159 (1995).
[22] J. Liu and G. Ahlers, Phys. Rev. E **55**, 6950 (1997).